JOURNAL OF CATALYSIS **106**, 313–317 (1987)

A Mathematical Model of the Channeling Activity of Metal Particles during a Catalyzed Oxidation of Graphite

Much has been speculated about the mechanism of the metal-catalyzed oxidation of carbon, based mostly on either the oxygen transfer or electron transfer mechanism. It was not, however, until recently that the cataytic activity of these metal particles was investigated in great detail using optical microscopy and controlled atmosphere electron microscopy (CAEM). Localized pitting on the graphite basal plane and subsequent channeling activity of metal particles at higher temperatures are commonly observed during the metal-catalyzed oxidation of carbon (*1–5*). Although the mobility of metal particles on graphite has been observed without any formation of pits or channels (*6, 7*), the channel propagation rate of a single catalyst particle is generally adopted as the basis for estimating the magnitude of the catalytic attack rate of graphite surface. It has been further shown from the CAEM studies by Baker and his co-workers (*3–5, 8*) that for a given temperature the channel propagation rate is inversely proportional to the square root of particle width in an oxidizing environment, whereas under reducing conditions the rate has a quadratic dependence with particle size. Baker and Sherwood (*8*) have proposed from these observations that in strong oxidizing conditions such as in the C–O_2 reaction, carbon atoms dissolved in the particle at the graphite–catalyst interface diffuse through a viscous outer layer of the particle and at the cooler face are converted to CO and CO_2 by reaction with oxygen, thereby creating a carbon concentration gradient in the particle. It is the purpose of this note to test the validity of the proposed mechanism on the metal-catalyzed oxidation of graphite just described above by setting up a mathematical model of the channeling activity of metal particles and comparing the theoretical results on the channel propagation rate with the experimental data available in the literature.

Here we consider a single isolated metal cube of length L, especially one in the platinum group, already establishing a steady-state channeling motion so that we neglect all transients associated with wetting, spreading and agglomeration of particles, intraparticle transport, etc. A schematic representation of the channeling activity is shown in Fig. 1. A two-dimensional view of carbon diffusion is assumed, since the particle is moving along the channel path and lateral diffusion is small compared to diffusion from the front face of the particle. Hence, carbon diffuses from the active catalyst–graphite interface, i.e., the front face, to the top surface where a thin viscous oxide layer is well established and provides a concentration gradient for carbon within the reduced metal matrix. It is assumed that unlike the metal particle, the thin oxide layer, consisting mostly of adsorbed oxygen atoms and diffused carbon atoms, cannot directly break carbon–carbon bonds. The thickness of the viscous oxide layer is small and remains constant throughout the steady-state motion of the particle. The existence of a surface platinum-oxide phase was identified by Chu and Ruckenstein (*9*) in their study of the kinetics of sintering of Pt crystallites on carbon substrates. It is likely that during a steady-state channeling motion of a particle, i.e., at a constant channel propagation rate, the rates of dissolution of carbon atoms at the metal–graph-

0021-9517/87 $3.00

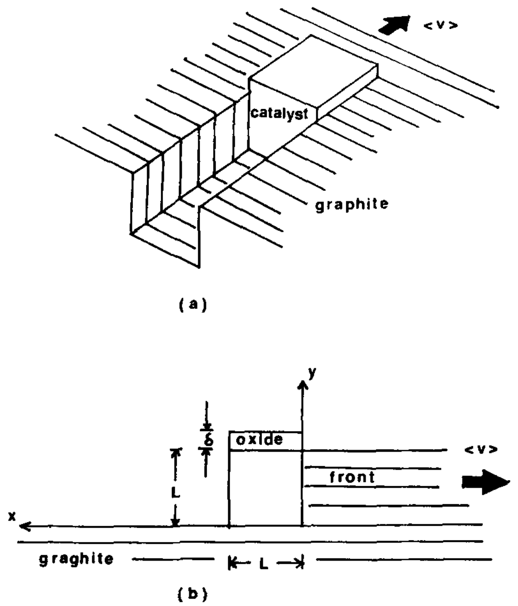

FIG. 1. Schematic sketch of the particle channeling activity model. (a) A general view, (b) a two-dimensional view.

ite interface, intraparticle diffusion of carbon atoms, and adsorption of oxygen atoms on the metal surface remain constant, if experimental conditions such as temperature and pressures including partial pressure of oxygen and the characteristics of the graphite surface such as the depth or height of an edge are kept constant. The rate of transport of carbon atoms from the bulk metal to the top surface of the oxide layer is hindered because of the presence of the thin oxide layer. This rate is proportional to the difference in concentrations of carbon at the metal–viscous oxide interface and at the surface. The proportionality constant is modeled by using a film theory where such a constant is determined by the diffusion coefficient of carbon atoms within the metal oxide and the oxide thickness, δ. The C–O_2 reaction only occurs within the oxide layer at the top surface, and when oxygen is in excess, it is assumed that the rate is first order in surface carbon concentration. Since the concentration of carbon within the oxide layer is distributed along the horizontal, its rate of consumption on the surface is not uniformly distributed so that both surface carbon concentration gradient and the mobile viscous nature of the oxide layer could impose a surface diffusion of carbon on the surface. It is further assumed that there is no diffusion and reaction of carbon behind the particle. Finally, although Baker and his co-workers contend a nonisothermal particle, it is regarded here as a first approximation that the particle is isothermal as well as the support.

Hence, for the metal matrix, the carbon balance equation becomes

$$D_{\mathrm{cm}}\left(\frac{\partial^2 c}{\partial x^2} + \frac{\partial^2 c}{\partial y^2}\right) = 0, \tag{1}$$

where c and D_{cm} are the concentration and the bulk diffusion coefficient, respectively, of carbon atoms within the metal matrix.

The boundary conditions for Eq. (1) are

$$c(0, y) = c_0 \tag{2}$$

$$\left.\frac{\partial c}{\partial x}\right|_{x=L} = 0 \tag{3}$$

$$\left.\frac{\partial c}{\partial y}\right|_{y=0} = 0 \tag{4}$$

$$-D_{\mathrm{cm}}\left.\frac{\partial c}{\partial y}\right|_{y=L} = K_{\mathrm{c}}\left(\left.c\right|_{y=L} - \bar{k}c^{\mathrm{s}}\right), \tag{5}$$

where c_0 is the solubility of carbon atoms in the metal, K_{c} is the mass transfer coefficient of carbon atoms through the metal–oxide layer interface, c^{s} is the surface concentration of carbon atoms in the oxide layer, and $\bar{k}$ is a thermodynamic constant relating the surface concentration to the volume concentration, assuming that there exists an equilibrium between carbon concentration in the metal resistive layer and the surface concentration in the oxide layer. As stated above, K_{c} is assumed to be $D_{\mathrm{c\text{-}mo}}/\delta$ according to the film theory, where $D_{\mathrm{c\text{-}mo}}$ is the diffusion coefficient of carbon atoms in the oxide layer. In Eq. (2), a solid-state reaction at the metal–graphite interface is represented by the dissolution of carbon atoms in the metal, rather than by the breakage of carbon–carbon bonds.

The surface carbon balance in the oxide layer is given by

$$D_{\mathrm{cs}} \frac{d^2 c^{\mathrm{s}}}{dx^2} - kc^{\mathrm{s}} - D_{\mathrm{cm}} \left.\frac{\partial c}{\partial y}\right|_{y=L} = 0, \qquad (6)$$

where D_{cs} is the surface diffusion coefficient in the oxide layer, and k is the first-order reaction rate constant. The boundary conditions for Eq. (6) are

$$c^{\mathrm{s}}(0) = c_0^{\mathrm{s}} \qquad (7)$$

$$\left.\frac{dc^{\mathrm{s}}}{dx}\right|_{x=L} = 0, \qquad (8)$$

where c_0^{s} is the saturation concentration of carbon atoms in the oxide layer. Since carbon atoms are likely to be supplied efficiently through the metal matrix to the oxide layer at $x = 0$, $c^{\mathrm{s}}(0)$ in Eq. (7) is assumed to maintain its saturation level. The last term in Eq. (6) represents the source for carbon atoms which is based on the assumption that during a steady-state channeling activity, all carbon atoms diffusing across the metal–oxide layer interface at $y = L$ have to reach the top suface of the oxide layer in order to maintain a constant oxide layer thickness and that the diffusion of carbon atoms within the oxide layer is one-dimensional, i.e., only in the y-direction, because the thickness δ is so small.

Equations (1) and (6) are coupled through Eq. (5), and analytical solutions for $c(x, y)$ and $c^{\mathrm{s}}(x)$ are possible by using the method of separation of variables. The solution procedure of this set of ordinary-partial differential equations is discussed in detail elsewhere (*10*).

Hence, the concentration profile for the carbon atoms in the metal matrix in a dimensionless form is given by

$$\mathbf{c}(\xi, \zeta) = 1 - 2 \sum_{n=0}^{\infty} \frac{\left(\frac{\tilde{k} c_0^{\mathrm{s}}}{c_0} - 1\right) \sin \lambda_n \xi \cosh \lambda_n \zeta}{\left(\frac{D_{\mathrm{cm}} \tilde{k} L}{D_{\mathrm{cs}}} - \frac{D_{\mathrm{cm}} k \delta L}{D_{\mathrm{cs}} \times D_{\mathrm{c\text{-}mo}}} - \frac{\lambda_n^2 D_{\mathrm{cm}} \delta}{D_{\mathrm{c\text{-}mo}} L}\right) \sinh \lambda_n - \lambda_n \cosh \lambda_n}, \qquad (9)$$

where $\mathbf{c}$ is the dimensionless concentration of carbon atoms, defined as c/c_0, $\xi = x/L$, $\zeta = y/L$, $\lambda_n = (2n + 1)\pi/2$, n is a positive integer, and δ is the thickness of the oxide layer as defined before.

And the surface concentration of carbon atoms in the oxide layer is given, in a dimensionless form, by

$$\mathbf{c}^{\mathrm{s}}(\xi) = \cosh \phi_2 \xi - \tanh \phi_2 \sinh \phi_2 \xi - \phi_3 \sum_{n=0}^{\infty} \frac{\tilde{A}_n \sin \lambda_n \xi}{\phi_2^2 + \lambda_n^2}, \qquad (10)$$

where $\mathbf{c}^{\mathrm{s}}$ is defined as $c^{\mathrm{s}}/c_0^{\mathrm{s}}$, $\phi_2 = (kL^2/D_{\mathrm{cs}})^{1/2}$, $\phi_3 = (D_{\mathrm{cm}} L c_0)/(D_{\mathrm{cs}} c_0^{\mathrm{s}})$, $\phi_1 = k_{\mathrm{c}} L/D_{\mathrm{cm}} = (D_{\mathrm{c\text{-}mo}} L)/(\delta D_{\mathrm{cm}})$, $\phi_4 = (\tilde{k} D_{\mathrm{c\text{-}mo}} c_0^{\mathrm{s}} L)/(D_{\mathrm{cm}} c_0 \delta)$, and $\tilde{A}_n = 2(\lambda_n \phi_4 - \phi_1)/(\phi_3 \phi_4 - \phi_2^2 - \lambda_n^2 - \phi_1 \lambda_n \coth \lambda_n)$.

The average flux of carbon atoms at the active metal–graphite interface is given by

$$-\langle v \rangle c_0 \mathbf{i} = \langle N_{\mathrm{c}} \rangle \mathbf{i}, \qquad (11)$$

where $\langle v \rangle$ is the channel propagation rate, $\langle N_{\mathrm{c}} \rangle$ is the average flux of carbon atoms, and $\mathbf{i}$ is the unit vector in the x-direction. The negative sign is inserted into Eq. (11) because the directions of the channel propagation and the flux of carbon atoms are opposite to each other.

Furthermore,

$$\langle N_{\mathrm{c}} \rangle = \frac{1}{L} \int_0^L N_{\mathrm{c}} \Big|_{x=0} dy = \frac{1}{L} \int_0^L - D_{\mathrm{cm}} \left.\frac{\partial c}{\partial x}\right|_{x=0} dy, \qquad (12)$$

where $N_{\mathrm{c}}|_{x=0}$ is the flux of carbon atoms at the front face of the metal cube.

The first-order rate constant, k, is evaluated by $k = k_0 \exp(-E/RT) = 10^{13} \exp(-80/1.987 \times 10^{-3} \times 1073) = 5.06 \times 10^{-4}\ \mathrm{sec}^{-1}$. Here, $E = 80$ kcal/mole at 800°C was obtained from the results by Otto and Shelef (*11*), and the pre-exponential factor was taken as $10^{13}\ \mathrm{sec}^{-1}$, a typical value for k_0. The surface diffusivity of carbon atoms, D_{cs}, was taken from the equation,

$$\begin{aligned} D_{\mathrm{cs}} &= 4.7 \times 10^{-2} \exp(-21 \times 10^3/RT) \\ &= 2.5 \times 10^{-6}\ \mathrm{cm}^2/\mathrm{sec}, \end{aligned}$$

experimentally obtained by Polak and Ehrlich (*12*) for nitrogen on the (110) plane of tungsten.

Assuming $L = 50$ nm, a typical value for active metal particles we now can approximate $kL^2/D_{\mathrm{cs}}\lambda_n^2 + 1 \simeq 1$ and $kL^2/D_{\mathrm{cs}}\lambda_n + \lambda_n \simeq \lambda_n$.

Using these approximations, substitution of Eqs. (9) and (12) into Eq. (11) and integration of the resulting expressions give the channel propagation rate as

$$\langle v \rangle = 2 \sum_{n=0}^{\infty} \frac{1 - \tilde{k} c_0^{\mathrm{s}}/c_0}{(\tilde{k} L^2/D_{\mathrm{cs}}) - (\lambda_n L/D_{\mathrm{cm}} \tanh \lambda_n) - (\lambda_n^2 \delta/D_{\mathrm{c\text{-}mo}})}. \tag{13}$$

It can be seen clearly from Eq. (13) that the channel propagation rate is inversely proportional to some quadratic form of particle size L, as observed experimentally (*3–5, 8*) and that the reaction kinetics of formation of CO and CO_2 in the oxide layer has no significant effect on the channel propagation rate. In order to compare the theoretical channel propagation rate above with the experimental data available in the literature, we further employ the following physical data. The diffusivity of carbon atoms in the metal matrix, $D_{\mathrm{cm}} = 2 \times 10^{-7}\ \mathrm{cm}^2/\mathrm{sec}$ was obtained from the high-temperature vacuum metallographic studies of carbon atom diffusion in metals by L'nyanoi (*13*). Due to the lack of data on the diffusivity of carbon atoms through the metal-oxide layer, $D_{\mathrm{c\text{-}mo}}$ was assumed to be roughly the same as D_{cs}, $2.5 \times 10^{-6}\ \mathrm{cm}^2/\mathrm{sec}$, and for the mathematical simplicity, the diffusion coefficients are assumed to be concentration independent. The solubility of carbon in platinum was taken as 10 atom%, based on the data by Ershov and Kasatkin (*14*). The concentration of carbon atoms at the active metal–graphite interface, c_0, was calculated to be about $1.1 \times 10^{-2}\ \mathrm{moles/cm}^3$, using the solubility data and the density of platinum of 21.4 g/ml. Assuming the effective thickness of oxide layer to be about 20 Å and knowing the density of carbon atoms of $2.26\ \mathrm{g/cm}^3$, the saturation concentration of carbon atoms in the oxide layer was calculated to be $4.0 \times 10^{-8}\ \mathrm{mole/cm}^2$. No data on $\tilde{k}$, defined previously as a thermodynamic constant relating the surface concentration of carbon atoms to the corresponding volume concentration in the oxide layer at equilibrium, seems to be available in the literature, and $\tilde{k}$ is roughly calculated to be in the range of $\sim 10^5\ \mathrm{cm}^{-1}$ for a monolayer coverage.

Plots of channel propagation rate versus particle width for different $\tilde{k}$ are shown in Fig. 2. For a fixed $\tilde{k}$, it is clear from Fig. 2 that there is an inverse relationship between channel propagation rate and particle width. Although the data by Baker et al. (*3*) are for palladium, there is an outstanding match between this model for $\tilde{k} = 2.7501 \times 10^5\ \mathrm{cm}^{-1}$ and their data, both qualitatively and quantitatively.

In conclusion, our preliminary model presented here is based on many simplifying assumptions such as steady-state channeling activity and isothermality of both metal particles and support, and lacks many thermodynamic considerations involved in this complicated solid–solid–gas heterogeneous reaction. However, the overall agreement between our theoretical results and experimental observations looks encouraging, and seems to further

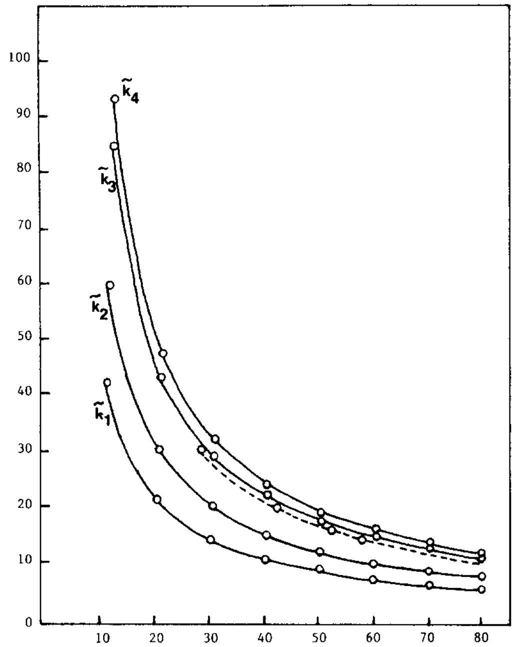

FIG. 2. Channel propagation rate predicted by model versus particle width. $\tilde{k}_1 = 2.75005 \times 10^5$ cm^{-1}, $\tilde{k}_2 = 2.75007 \times 10^5$ cm^{-1}, $\tilde{k}_3 = 2.75010 \times 10^5$ cm^{-1}, $\tilde{k}_4 = 2.75011 \times 10^5$ cm^{-1}, (---) = Baker *et al.* (*3*).

support the mechanism for the metal-catalyzed oxidation of carbon by oxygen proposed by Baker and Sherwood (*8*): the weakening of carbon–carbon bonds at the active metal–carbon interface and the dissolution of carbon atoms in the metal can be explained by the electron transfer mechanism, and the reaction between the diffused carbon atoms and the adsorbed oxygen atoms or molecules in the thin oxide layer indicates that an active catalyst is an oxygen carrier which perhaps undergoes a number of periodic oxidation–reduction cycles during the progress of reactions.

REFERENCES

1. Presland, A. E. B., and Headley, J. A., *J. Nucl. Mater.* **10,** 99 (1963).
2. L'Homme, G. A., Boudart, M., and D'Or, L., *Acad. R. Bull. Cl. Sci., Ser. 52* **5,** 1249 (1966).
3. Baker, R. T. K., France, J. A., Rouse, L., and Waite, R. J., *J. Catal.* **41,** 22 (1976).
4. Baker, R. T. K., Harris, P. S., Kemper, D. J., and Waite, R. J., *Carbon* **12,** 179 (1974).
5. Baker, R. T. K., and Chludzinski, J. J., Jr., *Carbon* **19,** 75 (1981).
6. Baker, R. T. K., Harris, P. S., and Thomas, R. B., *Surf. Sci.* **46,** 311 (1974).
7. Baker, R. T. K., and Skiba, P., Jr., *Carbon* **12,** 453 (1974).
8. Baker, R. T. K., and Sherwood, R. D., *J. Catal.* **70,** 198 (1981).
9. Chu, Y. F., and Ruckenstein, E., *Surf. Sci.* **67,** 517 (1977).
10. Choi, S. I., M.S. thesis, Michigan State University, 1984.
11. Otto, K., and Shelef, M., *Carbon* **15,** 317 (1977).
12. Polak, A., and Ehrlich, G., *J. Vac. Sci. Technol.* **14,** 407 (1977).
13. L'nyanoi, V. N., *Friz. Khim. Obrab. Mater.* **3,** 104 (1977).
14. Ershov, G. S., and Kasatkin, A. A., *Stal'* **8,** 712 (1977).

ALEXANDER S. CHOI

Department of Chemical Engineering
Michigan State University
East Lansing, Michigan 48824-1226

ANTONIO L. DEVERA

Rohm & Haas Company
7th Floor, Home Office
Independence Mall West
Philadelphia, Pennsylvania 19105

MARTIN C. HAWLAY

Department of Chemical Engineering
Michigan State University
East Lansing, Michigan 48824-1226

Received October 4, 1986